Chain Diffusion and Microstructure at a Glassy−Rubbery Polymer Interface by SIMS

H. C. Lin, I. F. Tsai, and A. C.-M. Yang*

Department of Materials Science and Engineering, National Tsing-Hua University, Hsinchu, Taiwan

M. S. Hsu and Y. C. Ling

Department of Chemistry, National Tsing-Hua University, Hsinchu, Taiwan

Received February 21, 2002; Revised Manuscript Received October 2, 2002

ABSTRACT: The microstructure and chain diffusion behavior at a rubbery/glassy polymer interface (PS/PPO) were studied using the depth-resolved technique of secondary ion mass spectroscopy (SIMS). Unlike the typical rubbery−rubbery interface, the microstructure of the miscible glassy−rubbery interface demonstrated a very sharp symmetric profile with a thickness around 25 nm before annealing. As chain diffusion took place, the glassy−rubbery interface moved toward the PPO region, the interface broadened asymmetrically, and the chains diffused across the interface showing both the Fickean and the case II characteristics simultaneously. For the purpose of analysis, the interfacial layer can be divided into a rubbery region and a glassy region according to the local T_g calculated from the local polymer concentration using the Flory−Fox equation. The case II characteristic dominated on the glassy side of the interface, where chain mass flow required plasticization of the glassy polymers by the neighboring rubbery chains. The Fickean characteristic, on the other hand, prevailed on the rubbery side of the interface, where polymers at both sides of the interface were rubbery chains. The effect of temperature on the interdiffusion was in good agreement with that predicted by the WLF equation. The average velocity of the interface decreased with the PS molecular weight following a negative power law. The power of the dependence, however, was different for the two molecular weight regimes above and below the critical molecular weight of PS (M_c = 38K). The mutual diffusion coefficient and the tracer diffusion coefficients were determined from the SIMS data. The results were in good agreement with the slow theory predictions.

Introduction

Polymer diffusion plays a very critical role in various segments of polymer technologies.[1−37] In polymer thin films and interfacial systems, the interfacial structure, strength, and dynamic properties are extremely sensitive to the polymer chain motions near the interfaces. Polymer diffusion is also a fundamental chain behavior from which the ultimate structure and dynamics of polymer chains can possibly be revealed. Following Alfrey, Gurnee, and Lloyd,[6] the general transport behavior of polymers is determined by the diffusion mobility relative to the relaxation rate of polymeric segments. The diffusion cases in which the rate of diffusion is much less than that of segmental relaxation, such as that of rubbery−rubbery interdiffusion in which the Fick's laws are obeyed, are classified as case I diffusion. Conversely, if the diffusion rate is more rapid than the segmental relaxation, the diffusion behavior is classified as following the case II diffusion characteristic.

The dynamic behavior of polymers in the melt has been successfully described by the reptation model,[1−3,5−7] in which the chain moves along a virtual tube defined by the environmental topological constraints imposed by the entanglements between the neighboring chains. For rubbery−rubbery interfaces, many research groups had explored the interdiffusion across the interface with various sample preparation and detection techniques.[8−37] Generally it is concluded that reptation model can be suitably used to describe the chain motions near the interface. The diffusion was found to depend on chain concentration, and error functions were used for the concentration profiles across the interfaces. On the other hand, the interfacial diffusion across a glassy polymer layer remains scarcely explored. Previously, Composto and Kramer,[19] using a special sample staining technique and the method of Rutherford back-spectroscopy (RBS), were able to obtain the diffusion profiles of the glassy−rubbery interfaces between the miscible polymers of polystyrene and poly(xylenyl ether; PXE). The data of interface movement pointed to a Fickian diffusion characteristic although the RBS results probably was suffered from a limitation of depth resolution and usually longer diffusion times were used for data collection. It was also revealed that the interdiffusion process was quite slow and the concentration profile was markedly asymmetric. The mutual diffusion coefficient of the glassy−rubbery interdiffusion was strongly dependent on the chain composition. Almost at the same time but slightly later, Sauer and Walsh[20] employed techniques of neutron reflection (NR) and spectroscopic ellipsometry (SE) to study the glassy−rubbery interface between polystyrene and poly(vinyl methyl ether). A sharp interface between the two polymers was found, which broadened gradually from 15 to 55 nm as diffusion proceeded. The interface moved with a constant velocity during the interfacial diffusion. These results, however, indicate a case II diffusion process[20] prevailing in the glassy−rubbery interface, in conflict with the RBS results reported by Composto and Kramer.[19]

To investigate the glassy−rubbery interdiffusion, we employed the SIMS technique here to study the polymer chain diffusion behavior at the interface of a miscible polymer pair: polystyrene (PS) and poly(2,6-dimethy1-1,4-phenylene oxide) (PPO). The diffusion in the polymer samples was controlled by annealing at a temperature

10.1021/ma020292j CCC: $25.00
Published on Web 03/13/2003

between the glass transition temperatures of the two polymers. As detailed in the literature, various experimental detection techniques were used to probe the interdiffusion across polymer interfaces. Among them, forward recoil spectroscopy (FRES),[18,32] infrared spectroscopy,[33] and small-angel neutron scatting (SANS)[26] can provide useful information for large interdiffusion depths but are limited by the depth resolutions to greater than 100 nm. Although neutron reflection (NR)[20,34] can provide high depth resolution but the samples require deuteration which may lead to additional problems of immiscibility and thermodynamic slowing down (TSD) due to the deuterium isotope effect.[22] In contrast, the secondary ion mass spectroscopy (SIMS)[38−43] is a very powerful and attractive technique for exploring polymer chain diffusion[21,22,35−37] In particular, it has excellent depth resolution of about 10 nm for element detection and is capable for direct concentration profiling of a given atomic species in a depth range up to several micrometers.[38] In this paper, the SIMS technique was used to study the polymer chain diffusion behavior at the rubbery−glassy interface of PS and PPO. The oxygen atoms bonded to the PPO backbones were used as "marker" for SIMS detection and accurate polymer concentration profiles were obtained. With the excellent depth resolution of SIMS, the microstructure of the glassy−rubbery interface and the characteristics of the interfacial diffusion, as well as the effects of temperature and PS chain entanglements were investigated.

Experimental Section

I. Sample Preparations. The diffusion sample consists of two layers of polymers, a 0.5 μm thick PS on top of a PPO layer of the same thickness, both supported by a polished silicon wafer. The PPO,[44] obtained from the Aldrich Chemical Co. (M_w = 244 000, M_n = 80 000), has a glass transition temperature of 500K. For the PS (M_w/M_n = 1.06, Pressure Chemical Co.), several molecular weights were used: 9000, 25 000, 90 000, and 2 000 000. The glass transition temperatures of the polymer ranges from 362 to 373 K according to the molecular weight. The PPO film was cast directly by spin coating from the toluene solution on a silicon wafer. The PS film was first cast by spin coating on a glass slide, and then floated onto a water surface, subsequently picked up onto the PPO layer that was already on a silicon wafer. For obtaining uniform PPO films, the solution was heated to approximately 373 K before casting. To remove the trapped water within the samples, the stacked films were dried in a vacuum at room temperature for least 24 h. For diffusion study, the samples were heated to an elevated temperature (393, 433, or 453 K) for various lengths of time. Under this annealing condition, the PS is in the rubbery state while the PPO is in the glassy state. Before the depth profile measurements, the sample was coated with a thin layer of gold (ca. 30 nm) to avoid electric charging.

II. SIMS. SIMS[38−42] has long been an important tool for material analyses. Recently, it has been frequently applied for studying polymer diffusion.[21,22,35−37] The basic principle of SIMS is using a primary ion beam to sputter secondary charged species, mostly secondary ions, out of the surface layer from a selected scanned area. The charged species are filtered through and counted by a mass spectrometer that is tuned to an element of interest. Repeated exposure of the same scanned area to the primary beam of constant current can be used to obtain the counts number of an element as a function of sputtering time, producing the useful data of depth distribution of the element of interest.

A secondary ion mass spectroscope (SIMS), CAMECA ims4f, was used to measure the depth concentration profile at the interfaces of the PS/PPO samples. The primary ion beam used was Cs^+, spot size around 30 μm^2, with an accelerating voltage of 13.5 kV maintained at a current of 26 nA. The scanned area is 225 μm by 225 μm. The produced secondary ions were analyzed for the elements of carbon ($13C^-$), hydrogen (H^-), and oxygen (O^-). At the beginning of each depth exploration, a transitional layer of 15 nm in thickness was usually required before a steady-state sputtering was reached. The thickness of the transitional layer, however, is less than that of the gold overcoat on each sample. Therefore, its effect on the concentration profile obtained from SIMS can be neglected.

Results

I. Quantitative Analysis of SIMS Data. The depth profile of the glassy−rubbery polymer interface can be probed and analyzed in details by using the SIMS technique. A typical set of raw data obtained from the SIMS depth profiling experiment is shown in Figure 1a presented in the format of secondary ions counts (hydrogen, oxygen, and carbon) vs the sputtering time. The sputtering rate was calibrated, and the raw data can be converted into the concentration profiles of the atomic species vs sample depth. The sputtering rates of PS and PPO were found to be quite similar, approximately 0.8 nm/s. The depth resolution of the concentration profiles is around 10 nm. The major source of resolution limitation in SIMS comes from the instrumental broadening. Since the PPO chains contains oxygen atoms while the PS chain has no oxygen atom at all in its chemical structure, the oxygen ions current was used for probing the depth concentration profile of the PPO molecules. However, before an accurate quantitative diffusion analysis can be made, the experimental artifacts due to contaminations were to be identified and eliminated from the SIMS raw data. First, the existence of a conspicuous peak in the oxygen profile near the free surface, as shown in Figure 1a, was frequently observed, and it was identified as due to the adsorbed water from the ambient storage environments. A similar anomalous peak was also usually present at the PS−PPO interface before annealing, also shown in Figure 1a. Upon annealing, this peak moved to the free surface as shown in Figure 2. The moving speeds of this peak at different annealing temperature were measured and the activation energy Q was determined to be around 8.4 J/mol, very close to that reported for water vapors in polymers.[45] The peak was hence attributed to the humidity vapors trapped during sample preparations where a water floating process was used. These peaks were generally ignored for diffusion data analysis.

For quantitative determination, the oxygen ion counts were first normalized according to the carbon ion counts of the same sample. A typical result is shown in Figure 1b. To obtain the PPO volume fraction, φ_{PPO}, from the SIMS data, a relative sensitivity factor, β (atoms/cm^3), was defined according to $\rho_i = \beta(I_i/I_m)$, where I_i is the secondary oxygen ion intensity and I_m is the intensity of the matrix carbon isotope secondary ions (counts/s). The theoretical value of the ratio I_i/I_m is $^1/_8$ for PPO polymer; the factor β can be empirically determined using the SIMS experimental values of I_i/I_m obtained from a pure PPO sample. The value of β was then used to convert the SIMS data of the diffusion samples into the depth profile of φ_{PPO}. A typical PPO concentration profile of a PPO/PS sample before annealing was demonstrated in Figure 1c where it was shown that the PPO concentrations in the PS and the PPO bulk regions were generally flat. The precise interfacial position and the diffusion coefficient were determined using the Boltzmann−Matano analysis.[19,46,47]

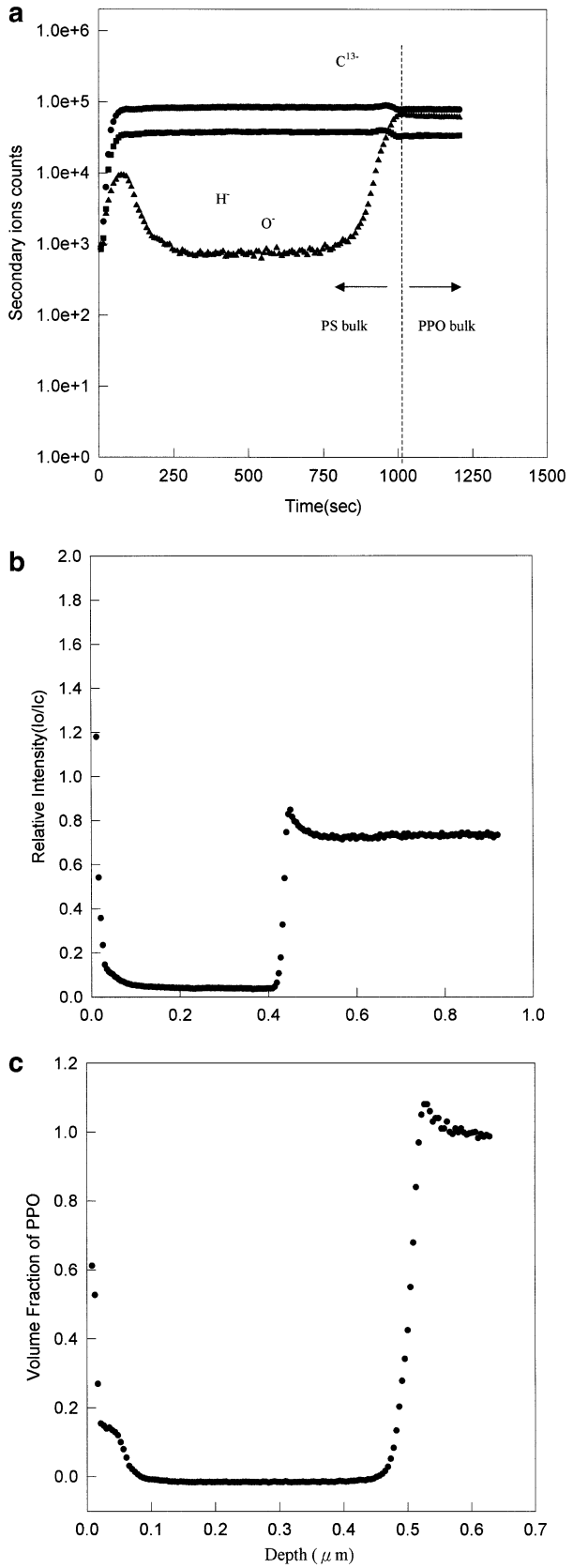

Figure 1. Diffusion profile of a 90KPS/ PPO diffusion couple from SIMS experiments before annealing: (a) the raw data, (b) the relative intensity profile of oxide ions, and (c) the PPO concentration profile.

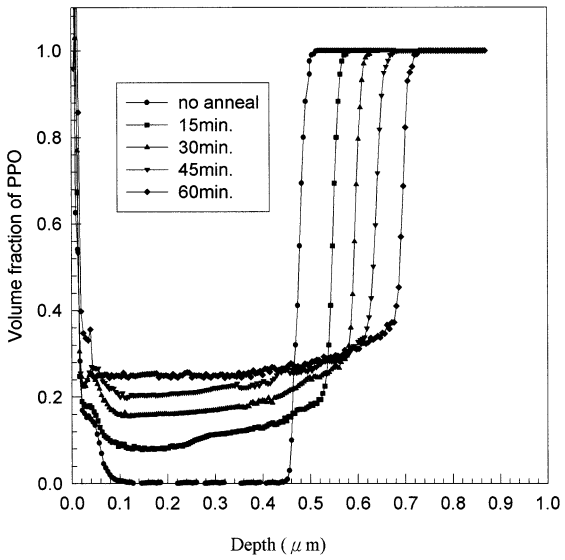

Figure 2. PPO concentration profile of 90KPS/PPO diffusion couple annealed at 453 K for 15, 30, 45, and 60 min.

II. General Diffusion Behavior at the Rubbery—Glassy Interface. Figure 2 shows the PPO depth profile before annealing. The depth profile of the interface is quite symmetric with respect to the Matano plane at which the concentration profile showed a very sharp transition from φ_{PPO}= 1.0 to φ_{PPO} = 0.20 over a thin transition zone with a thickness around 20−30 nm. After the sample was annealed at 453 K, the depth profile changed into an asymmetric distribution with a Fickean diffusion profile appearing in the PS side of the interface. The Fickean diffusion profile apparently was due to the PPO chains diffused across the interface. Other than the Fickean diffusion profile in the PS side of the interface, the PPO concentration in the PS bulk is approximately constant with depth. On the other hand, the concentration profile at the PPO side of the Matano interface remained very steep. The PPO concentration in the PPO bulk was undiluted with the rubbery PS molecules and maintained at a constant level of φ_{PPO} = 100%. This observation is in good agreement with that reported previously by Composto and Kramer in a similar system using Rutherford back spectroscopy (RBS).[19]

Concurrent to the evolution of the depth profile across the interface during polymer interdiffusion, the Matano interface was moving toward the PPO bulk. The interdiffusion effectively resulted a progressive thinning of the PPO bulk. As the interdiffusion proceeded, the PPO concentration in the PS bulk increased steadily, in a sharp contrast to the observation that the PPO volume fraction in the PPO bulk always remained fixed at around 100%. The fact that the PPO concentration in the PS bulk is approximately constant indicates that the PPO molecules exiting from the interface quickly dispersed within the PS bulk uniformly. The driving force behind the quick PPO dispersion is believed mainly to be due to the large negative enthalpy of mixing of the two polymers.

The sharp PPO concentration profile at the PPO side of the interface strongly indicates the case II diffusion dominance at the location. In that, the glassy PPO layer located at the interface was first plasticized by the nearest neighboring PS chains which, driven by the free energy of mixing, subsequently started to diffuse into the thin plasticized PPO region. When sufficient PS segments had diffused into the plasticized PPO layer, individual PPO chains were then able to undergo higher order chain motions, to be “dissolved“ from their ho-

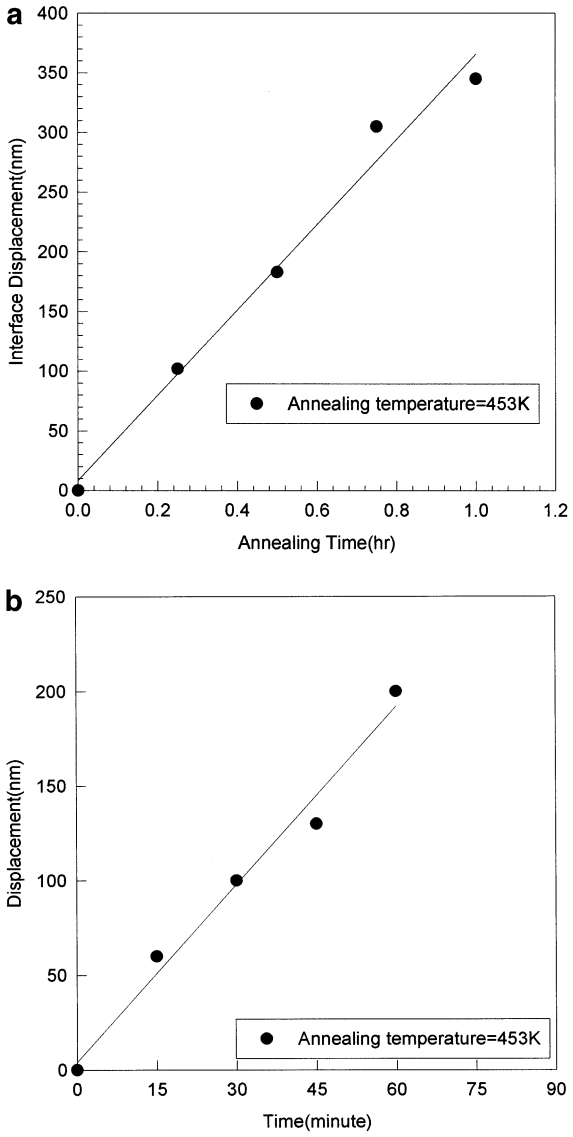

Figure 3. Matano interface displacement vs annealing time at 453 K for (a) diffusion couple 9KPS/PPO and (b) diffusion couple 90KPS/PPO.

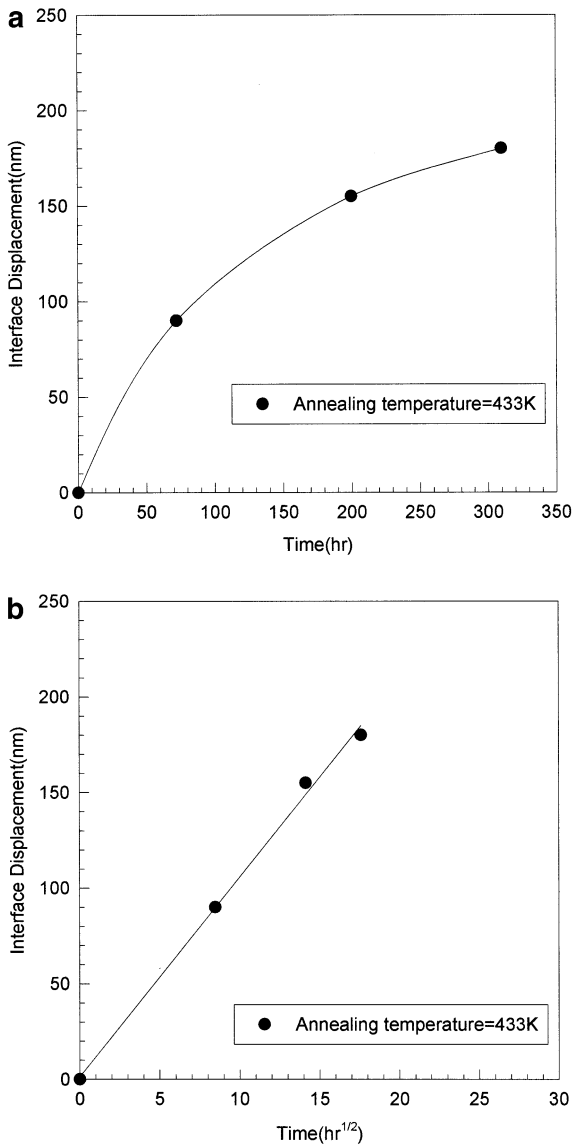

Figure 4. (a) Matano interface displacement vs annealing time of the diffusion couple 90KPS/PPO at 433 K. (b) Matano interface displacement vs the square root of annealing time of the diffusion couple 90KPS/PPO at 433 K.

mopolymer glassy entanglement network, and to diffuse into the rubbery PS layer. The thickness of the steady-state plasticized interfacial region, as indicated by the SIMS depth profile data, is very thin, on the order of less than 20 nm. However, this interface, as will be shown later, eventually grew into a macroscopic scale when the interdiffusion across the PS/PPO interface finally approached an equilibrium state.

As shown in Figure 2, the diffusion of the PPO chains into the rubbery PS bulk created a Fickean diffusion profile at the PPO side of the interface. The Fickean process is widely regarded as the dominant diffusion mechanism in polymer melts. As was correctly pointed out by Sauer and Walsh,[20] the PPO diffusion into the PS bulk in fact is similar to the dissolution of glassy polymer in a good solvent. In summary, it is apparent that according to the SIMS data the PS chains moved into the PPO bulk following a case II diffusion while the PPO molecules permeated into the PS bulk in a fashion governed by a Fickean diffusion process. The SIMS depth profile of the glassy/rubbery interface clearly demonstrates these two characteristics simultaneously.

The moving velocity v of the PPO/PS interface toward the PPO bulk was found to be approximately constant for short annealing times. The data are shown in Figure 3. This was also when the PPO concentration across the interface did not change too significantly from that in the unannealed samples. At longer diffusion times, the interface velocity v started to slow, resulting in a deviation from the linear relationship of v vs t, as shown in Figure 4a. The deviation of linearity of v vs t became significant when the PS bulk had been heavily diluted by the PPO molecules that migrated across the PPO/PS interface, and the interface velocity v started to show a linear dependence on the square root of diffusion time t, as demonstrated in Figure 4b. Nevertheless, the concentration profile across the interface remained very steep and the PPO concentration in the PPO bulk was always undiluted at 100%. Therefore, the slowdown of the interface movement does not correspond to a change of the chain diffusion mechanisms. Instead, it was attributed to a decrease of the chemical potential differences of the polymer molecules across the glassy/rubbery interface. The interface slowdown is related to

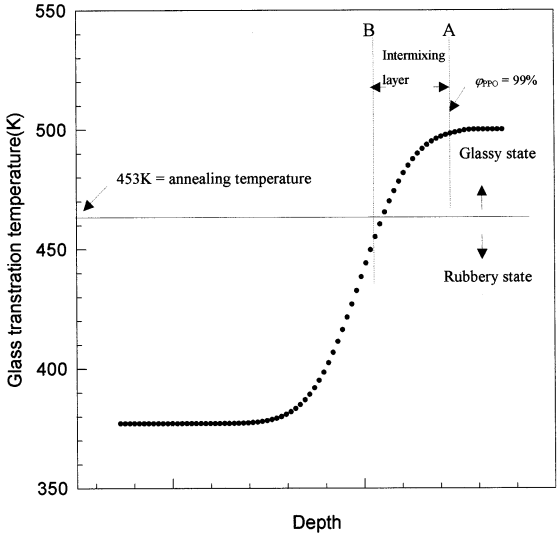

Figure 5. Schematic diagram of the PS/PPO interfacial microstructure that shows the intermixing layer.

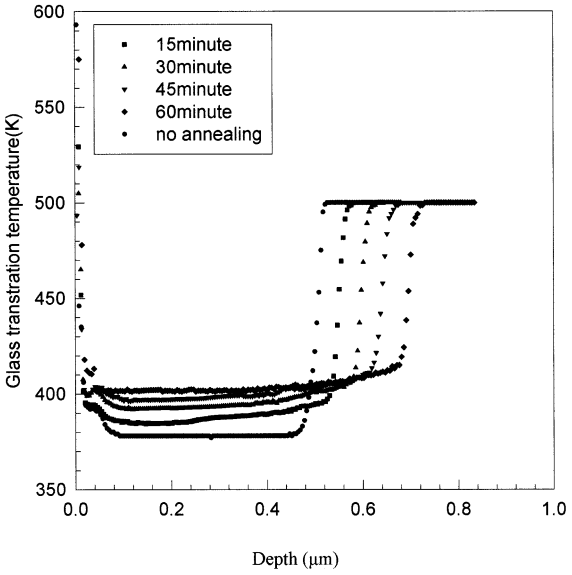

Figure 6. Local effective glass transition temperature distribution vs depth of thediffusion couple calculated from the SIMS PPO concentration profiles (90KPS/PPO at 453 K).

the broadening of the interface and the analysis will be shown in the Discussions.

III. Microstructure of the Glass—Rubber Interface. For convenience of analysis, the layer between the plane $\varphi_{PPO} = 0.99$ (plane A), schematically shown in Figure 5, and the plane where the tangent of the PPO concentration profile in the PS bulk intercepted with $\varphi_{PPO} = 0$ was defined as the interfacial region at the PPO/PS interface. The structure and properties of the interfacial layer can be resolved spatially from the composition profile provided by SIMS experiments. Since PPO and PS are miscible over the full concentration range, it was assumed that in the interfacial layer the PS and PPO chains mixed homogeneously down to the molecular scales such that a single T_g could be locally assigned. The local T_g distribution in the interfacial layer was calculated using the Flory−Fox equation from each concentration profile acquired from the SIMS experiments. The results are shown in Figure 6. To test the validity of the Flory−Fox equation, a PPO/PS blend (60%/40%) was prepared and its T_g was

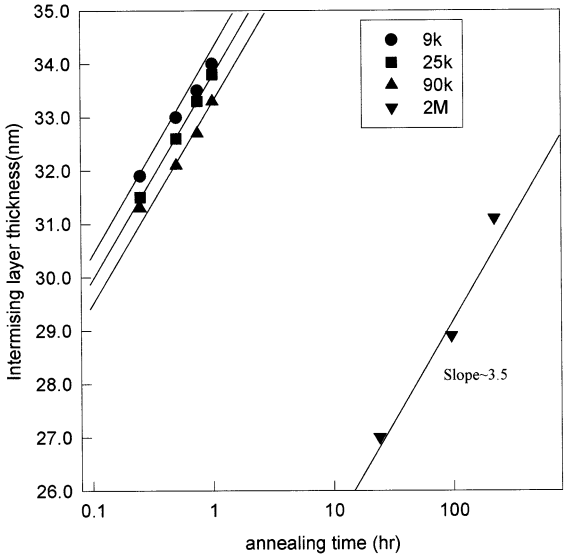

Figure 7. Intermixing layer thickness vs annealing time at 453 K for various PS molecular weights (slope ~ 3.5).

determined using a differential scanning calorimeter (DSC). The DSC result was approximately 407 K, very close to that predicted using the equation. For each curve in Figure 6, the interface can be conveniently divided into a rubbery layer and a glassy layer by a plane (the plane B) at which the local T_g is equal to the annealing temperature. Corresponding to the annealing temperature 453 K, the PPO concentration *at* plane B is $\varphi_{PPO} = 0.66$. The rubbery layer (resided on the PS side of the interface) in fact was the gateway for the PPO molecules to diffuse into the PS bulk. Since they were rubbery, the polymer chains in this region were free to move and should obey a Fickean diffusion process according to the results of the numerous previous studies.[18,28] This is also in good agreement with the SIMS depth profile which shows a Fickean diffusion profile in the rubbery interfacial region. On the other hand, the glassy layer (resided on the PPO side of the interface) was a region filled with partially plasticized PPO molecules and the incoming PS chains. Hence, a term "intermixing layer" was used for this interfacial region. This glassy layer is very thin, on the order of 20−30 nm. The sharp PPO gradient at the intermixing layer strongly indicated an interdiffusion dominated by the individual PPO molecules that were plasticized and "dissolved" from the glassy PPO matrix permeating across the interface rather than by the collective movement at the interface of the whole entangled PPO chain mass gradually swollen by the plasticizing PS front. Beyond the Fickean diffusion profile that was extending several hundreds nanometers from the intermixing layer on the PS side of the interface, the PPO concentration was quite constant in the PS bulk. This indicated a very fast dispersion of the PPO chains in the PS bulk due to the quite negative χ interaction parameter. The rapid dispersion further supported the assertion that the migration of the PPO molecules into the PS bulk was consist of molecular motions of individually dissolved chains rather than that of the whole PPO entanglement network.

The intermixing layer was found broadening as the interdiffusion proceeded, however. As the annealing time increased, the intermixing layer thickness increased steadily, as shown in Figure 7. As correctly pointed out by Sauer and Walsh,[20] the change in the

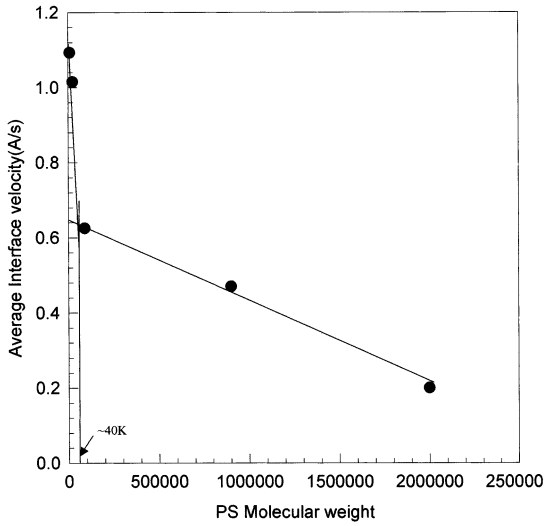

Figure 8. Matano interface velocity vs PS molecular weight for 1 h annealing at 453 K.

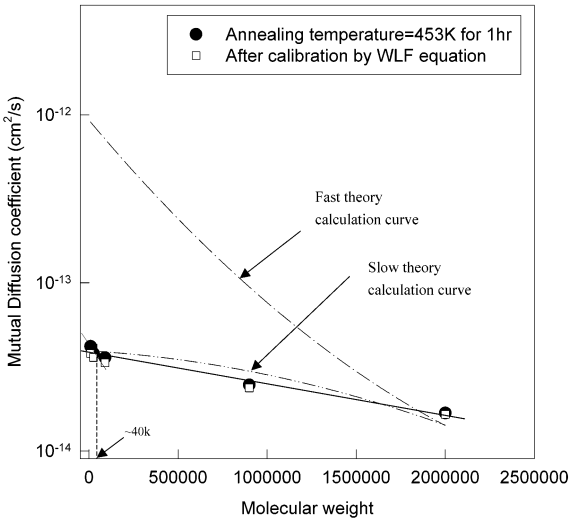

Figure 9. Mutual diffusion coefficient determined from SIMS data vs PS molecular weight. The circles are data normalized with the glasstransition by WLF equation and the squares are the original data calculated from eq 3. The dashed lines are calculations from the "slow theory" and "fast" theory.

intermixing layer thickness is due to the velocity differential between the interfaces A and B (illustrated in Figure 5), which were both moving toward the PPO bulk during interdiffusion. The movement of plane A was controlled by the rates of plasticization and permeation of individual glassy PPO chains from the PPO bulk, a process restricted by the case II diffusion of PS into the PPO bulk. Since φ_{PPO} on both sides of plane A was approximately invariant with time, the velocity of plane A was approximately constant during the entire course of interdiffusion. On the other hand, the movement of the plane B, resulted from the interdiffusion of the fully plasticized PPO chains and the PS bulk (a Fickean diffusion), was strongly influenced by the gap of chemical potential of PPO chains across the plane B, and hence decreased with annealing time. Therefore, broadening inevitably takes place in the interdiffusion across the glassy−rubbery polymer interface.

IV. Effect of Temperature and the PS Molecular Weight. The movement of the Matano interface during annealing was strongly influenced by the annealing temperature. As shown in Figure 4, the moving velocity of the interface increased significantly as the annealing temperature increased from 433 to 453 K. The values of the interface moving velocity v_{433} and v_{433} (corresponding to the diffusion at the annealing temperatures 433 and 453 K) are in good agreement with the prediction of the WLF equation, i.e., $\log (v_{433}/v_{453}) = \log a_T = C_1(433\text{ K} - 453\text{ K})/C_2 + (433\text{ K} - 453\text{ K})$, where the universal constants are $C_1 = -17.44$ and $C_2 = 51.6$.

The interface velocity was also found to be strongly influenced by the PS molecular weight. The experimental results of the interface velocity, averaged up to 1 h diffusion time, vs PS molecular weight are shown in Figure 8. The velocity decreased with the PS molecular weight according to a negative power law in each of the two molecular weight regimes divided by the critical molecular weight of PS ($M_c = 38$K). The observed effect of PS molecular weight was attributed to two contributions. First, longer polymer chains require longer times to penetrate and plasticize the PPO chains, leading to slower chain interdiffusion. Second, when the PS chains become longer than the critical molecular weight M_c, chain entanglements form and reduce the chain mobility of both the PS and PPO chains. When the PS chain length is greater than M_c, the plasticization in the intermixing layer becomes less effective, and the PPO chains in the intermixing layer are further constrained by the entanglement network of PS and, according to the reptation model, need to undergo repetitive worm-like motions along the "tube" to result a net coil displacement.

The mutual diffusion coefficient D was calculated using the Matano method[6,19] at $C_{PPO} = 0.5$:

$$D = -\frac{1}{2t}\frac{\partial x}{\partial C_{PPO}}\int_0^{0.5} x\, dC_{PPO} \quad (1)$$

where D is the mutual diffusion coefficient at the PPO concentration $C_{PPO} = 0.5$ at the annealing temperature T_a, t is the annealing time, x is the position of C_{PPO}, and the integral item is the inverse slope of the concentration profile. Apparently, the calculated results are highly dependent on the concentration profiles determined experimentally. The concentration profiles (t = 1 h) determined by SIMS were used to calculate D. Figure 9 shows the mutual diffusion coefficient obtained by using eq 1 as a function of the PS molecular weight. It is clear that the diffusion coefficient follows the same trend as that of the interface velocity. That is, at both the low molecular weight and high molecular weight regimes divided by the PS entanglement molecular weight (M_e = 19K), the mutual diffusion coefficient decreases in a simple power law with the PS molecular weight. The molecular weight of the PS, however, has an effect on the T_g of PS. For the sake of comparison, the effect of molecular weight on the T_g of PS chains was calibrated by analyzing the diffusion coefficient evaluated at a $T - T_g = 80$ K. This was be done by shifting the D's according to the WLF equation using the shift factor a_T defined as the ratio of the diffusion coefficients D to D_{T_g+80}, corresponding respectively to the diffusion coefficients at the annealing temperature T_a and the temperature $T_g + 80$

$$\log a_T = \log\left(\frac{D}{D_{T_g+80}}\right) = \frac{C_1[T_a - (T_g + 80)]}{C_2 + [T_a - (T_g + 80)]} \quad (2)$$

Figure 9 also shows the shifted results of the mutual

diffusion coefficient with various PS molecular weights. The differences between the shifted data of D_{T_g+80} and the original values of D, however, are quite small and can be neglected.

Since the mutual diffusion coefficient D is controlled by the excess enthalpy and entropy of segment−segment mixing, D can be expressed in terms of the Flory−Huggins χ interaction coefficient and the segment mobilities of polymers. Following the results developed by Brochard, Jouffroy, and Levinson,[7] consider a regular solution of chemically dissimilar polymers A and B, each with degrees of polymerization N_A and N_B and the Onsager coefficients Λ_A and Λ_B (defined by the flux equations), respectively. The Onsager coefficients can be related to the segment mobilities as follows $\Lambda_A = \varphi_A\Lambda_{0A}$ and $\Lambda_B = \varphi_B\Lambda_{0B}$ where Λ_{0A} and Λ_{0B} are the segment mobilities of the polymer components represented by the subscripts. It can be shown that for the simple case of a symmetrical blend ($N_A = N_B = N$, $\Lambda_{0A} = \Lambda_{0B}$) the mutual diffusion coefficient D can be expressed in the context of a lattice model as[9]

$$D = 2(\chi_s - \chi)\varphi_A\varphi_B D_T \tag{3}$$

for nonentangled short chains where χ_s is the interaction parameter at the spinodal point and D_T is the segmental diffusion coefficient of the interdiffusion. For entangled long chains, an additional factor of N_e/N, where N_e is the threshold value of N to have entanglements, should be multiplied on the right-hand side of the equation to include the reptation effect. The interaction parameter χ_s can be expressed by the equation[18]

$$\chi_s = [(N_A\varphi_A)^{-1} + (N_B\varphi_B)^{-1}]/2 \tag{4}$$

Brochard et al.[9] and Binder[10] had postulated that incompressibility condition occurred during diffusion, thus the fluxes of the diffusing species at the interface should be equal in value and opposite in direction. Therefore, the mutual diffusion coefficient is controlled by the diffusion of the slower moving component if the two components have very different mobility. This is the so-called "slow theory", in which D_T becomes[18]

$$\frac{1}{D_T} = \frac{\varphi_B}{D_A{}^*N_A} + \frac{\varphi_A}{D_B{}^*N_B} \tag{5}$$

where $D_A{}^*$ and $D_B{}^*$ are the tracer diffusion coefficients of the A and B polymer segments according to the Rouse theory. The tracer diffusion coefficients of the segments can be expressed as[28]

$$D_A{}^* = \frac{kT}{\xi_A N_A} \quad \text{and} \quad D_B{}^* = \frac{kT}{\xi_B N_B}$$

where ξ_A and ξ_B are the segmental friction coefficients of polymers A and B, respectively, and k is Boltzmann's constant. However, the condition of volume impressibility becomes unnecessary, as pointed out by Kramer, with the introduction of a vacancy flux in the interdiffusion in a lattice model allowing a bulk flow across the interface. In this approach, Kramer derived that D_T can be expressed as[18]

$$D_T = \varphi_B D_A{}^* N_A + \varphi_A D_B{}^* N_B \tag{6}$$

which, also in agreement with the independent work by Sillescu,[11,12] indicates an interdiffusion-controlled by the fast moving component and hence is called the "fast theory".

Although the majority of the previous research work concerning identifying either the "slow theory" or the "fast theory" to be the dominant mechanism in a interdiffusion was confined within the realm of rubbery−rubbery interfaces, it is interesting to analyze our data in the light of the above theories in order to gain insights into the relatively unexplored glass−rubbery interdiffusion. The mutual diffusion coefficients D determined from the SIMS profiles using eq 1 were compared with the theoretical values from eq 3 using respectively the segmental diffusion coefficient D_T's calculated from the slow theory (eq 5) and the fast theory (eq 6) for different PS molecular weights in the PS/PPO diffusion couple with the Flory−Huggins interaction parameter[44] $\chi = -0.024$. In the calculations of D_T's, the tracer diffusivities of PS and PPO measured by Composto and Kramer[18] at 479 K ($D^*_{PS} \sim 3 \times 10^{-12}$, 5×10^{-13}, 9×10^{-14}, 9.2×10^{-16}, and 9×10^{-17} for MW = 9000, 25 000, 90 000, 900 000, and 2 000 000 respectively, and $D^*_{PPO} \sim 7.65 \times 10^{-16}$) were used after a WLF conversion for normalizing the temperature difference with our experiment here. The calculations were compared with the SIMS data as shown in Figure 9. The measured diffusion coefficients are generally on the order of 10^{-14}cm^2/s, following closely the "slow theory" calculations. In our diffusion experiment, the PPO chains, the slow component, were initially frozen and required the plasticization of the mobile PS chains to activate the interdiffusion across the interface. Therefore, the interdiffusion was in fact controlled by the plasticization rate and movement of PPO chains. Only when the PPO chains at the interface were swollen and started to diffuse, the PS chains can diffuse into the PPO layer.

The broadening of the intermixing layer with the diffusion time t_d followed an empirical rule, $\tau = k \ln t_d$ where k is a constant independent of the PS molecular weight. The data were shown in Figure 7 where the broadening curves for the different PS molecular weights are parallel to each other. For a given diffusion time t_d, the intermixing layer is thinner for the higher PS molecular weight, probably due to slower interdiffusion. Attempts to shift these curves in Figure 7 by normalizing the T_g difference using the WLF equations, however, failed. At least it implies that for the interdiffusion involving different PS molecular weight the interfacial broadening does not follow the same mechanisms. For instance, as the molecular weight of PS increased from 9K to 2000K, molecular chain motions may change from that following the Rouse model to that described by the reptation model.

V. Diffusion toward the Equilibrium Stage. As the diffusion time increased, the concentration profile of the polymer across the interface became more and more gentle and eventually leveled. The glassy−rubbery interface finally evolved into the equilibrium configuration. Figure 10 shows the PPO concentration profile of PS(90K)/PPO at 433 K after 310 h of annealing. The concentration profile demonstrates an interfacial layer thickness of around 100 nm. It is somehow surprising to note that when the concentration profile finally leveled, the calculated local T_g became greater than the annealing temperature, 433 K. As mentioned before, the chain mobility at the interfacial region can be estimated

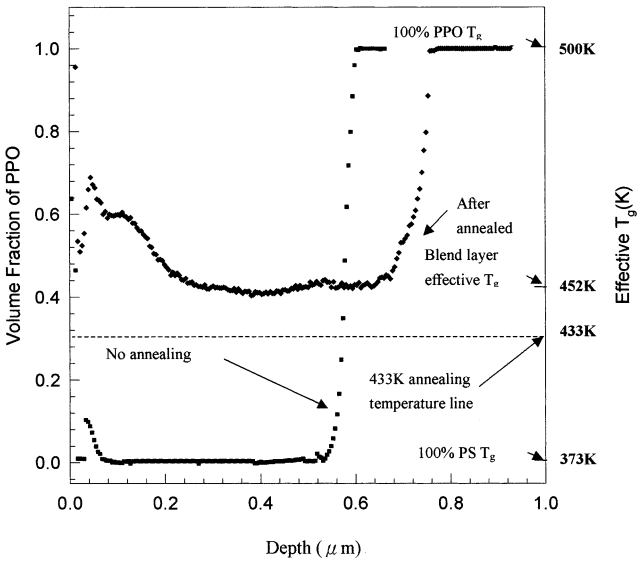

Figure 10. Concentration profile of 90KPS/PPO) annealed for 310 h at 433 K.

from the local effective T_g. Thus, the interdiffusion across the glass−rubber interface should cease to occur and the interface became stationary when the local T_g is equal to or greater than the annealing temperature. However, it was found otherwise (Figure 10). This observation will be discussed later.

Discussions

Our data revealed that the chain concentration gradient across the glassy−rubbery interface was very sharp for short diffusion times. The sharp interfacial gradient broadened very slowly with diffusion time. This behavior is very different from that of the rubbery−rubbery interdiffusion reported previously where the interface broadened quite rapidly with diffusion time. In addition, the Matano interface of the rubbery−glassy diffusion moved much faster than that in the rubbery−rubbery diffusion, obviously due to the large differentiation between the chain diffusivities on the both sides of the interface. The apparently complex behavior of polymer interdiffusion across a glassy−rubbery interface, however, can be deciphered and analyzed in details by identifying the "intermixing layer" residing at the interface. As defined in the previous sections, the "intermixing layer" is where the glassy, immobile PPO chains being plasticized by the rubbery PS molecules at the glassy−rubbery interface. The width of the "intermixing layer" is very small, on the same order of magnitude as the radius of gyration of the glassy macromolecules. It is clear from the data that the plasticization process of the PPO chains by the PS molecules preceded the advancement of the PS into the PPO bulk, constructing a case II diffusion behavior for the PS chains into the PPO layer. This assertion is strongly supported by the following facts. First, the PS diffusion front into the PPO matrix was very sharp and the PPO concentration behind this front always kept undiluted at $\varphi_{PPO} = 100\%$. Also, the PS diffusion front traveled toward the PPO bulk with a constant velocity at short diffusion times when the PPO concentration difference across the interface did not change markedly. This process in fact is strikingly similar to the dissolution of a glassy polymer in a "rubbery" good solvent. In the conventional case II diffusion cases small molecules were absorbed up in a polymer where the small molecules can penetrate the bulk without the removal of the macromolecules from their occupied space. The advancement of PS front here, proceeded with a slow speed around 0.05 nm/s, requiring not only the plasticization of the PPO molecules but also, very likely, the removal of the plasticized PPO molecules from the PPO bulk to yield room for the incoming PS molecules. Under the condition of volume incompressibility, the sharp diffusion front case II diffusion should be compounded with the effects produced by the diffusion of the dissolved PPO macromolecules into the PS bulk. The migration of the plasticized PPO chains into the rubbery PS bulk, the PPO removal process, obviously followed a Fickean diffusion behavior in that the PPO concentration profile at the PS side of the interface illustrated a typical Fickean profile, consistent with the well-held conclusion in the literature that in polymer melts polymer chains transported following Fickean diffusion. The fully plasticized PPO molecules had demonstrated a high mobility in that once they permeated through the interface they quickly dispersed uniformly into the PS bulk. In summary, the interdiffusion across the glassy−rubbery interface in fact demonstrates both case II and Fickean characteristics simultaneously.

One important ramification can be drawn from the SIMS observations. Under the condition of volume incompressibility, the sharp interface indicated an unreasonably high swelling ratio of the PPO entanglement network at the interface if no chain disentanglement was allowed for the PPO chains. For instance, given an interface profile of concentration variation from $\varphi_{PPO} = 1.0$ to $\varphi_{PPO} = 0.2$ over a thickness around 25 nm ($t_a = 15$ min, Figure 2), the swelling ratio under the above conditions would be approximately 5, exceeding the maximum elongation extension ratio $\lambda_{max} = 3.0$ that the PPO entangled strands[48] can withstand. Also it was observed that the dissolved PPO molecules quickly dispersed uniformly and reached the other end of the PS bulk. Therefore, the plasticized PPO chains within the intermixing layer must have completed the dissociation process from their glassy chain network before permeation into the PS bulk.

The disentangled and fully plasticized PPO chains would quickly dissolve into the PS bulk, apparently due to the large negative enthalpy of mixing with the PS chains, leaving behind a sharp PPO concentration gradient at the glassy−rubbery interface of a thickness comparable to the radii of gyration of PPO molecules.

The concentration profile across the glassy−rubbery interface obtained from the SIMS experiments provides the structural information on the diffusion front, e.g., the identification of the intermixing layer. The SIMS data, however, was intrinsically coupled with a broadening effect stemming from the SIMS instrumentation. It is desirable to deconvolute this broadening effect in order to obtain more accurate information on the interfacial microstructure. For this purpose, it is a reasonable approximation that the actual concentration depth profile $c(z)$, the SIMS broadening function $g(z)$, and the SIMS measurement $I(z)$ satisfy the following relation[41,42]

$$I(z) = \int_{-\infty}^{\infty} c(z')g(z - z')\,dz' \qquad (7)$$

In addition, a step function was assumed for the actual depth profile $c(z,t)$ before interdiffusion taking place, i.e.,

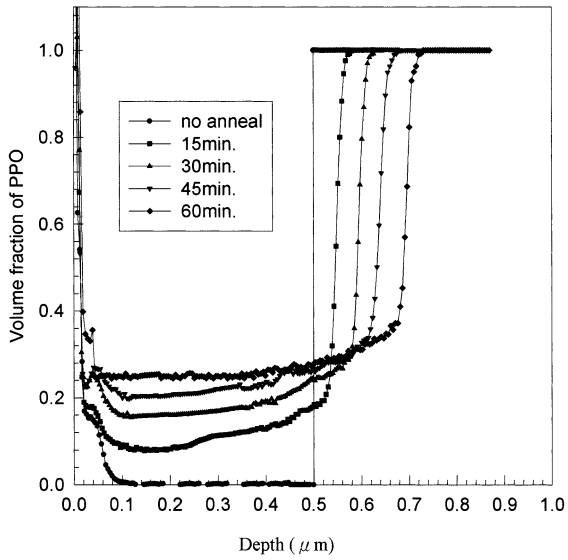

Figure 11. Concentration profiles of 90KPS/PPO at 453 K for various annealing times after deconvolution.

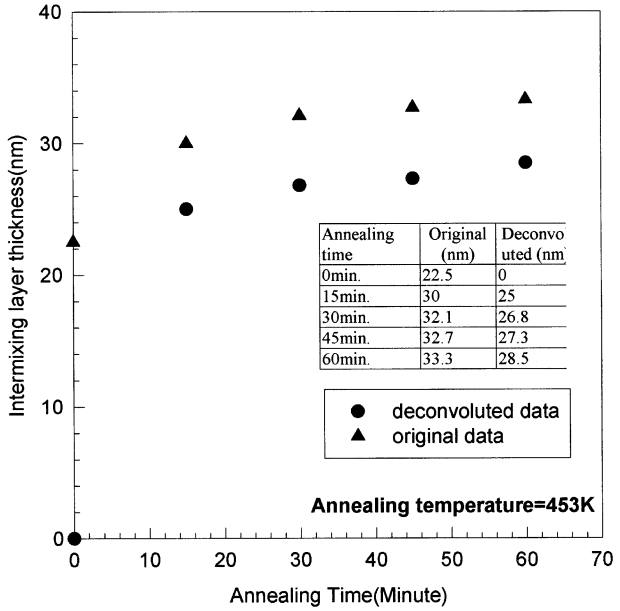

Figure 12. Intermixing layer thickness vs the annealing time.

$c(z, t = 0) = 0$ in the PS bulk and $c(z, t = 0) = 100\%$ in the PPO bulk. Thus, the SIMS broadening function $g(z)$ could be calculated from eq 7 using the SIMS data $I(z, t = 0)$ of the unannealed samples. The broadening function $g(z)$ was then used to calculate the actual concentration profile $c(z)$ via a deconvolution process based on eq 7. The deconvoluted profiles $c(z)$ of the PS(90K)/PPO for various annealing times are shown in Figure 11. The thickness of intermixing layer of the corresponding profile was determined and shown, along with that from raw data $I(z)$, in Figure 7. The deconvoluted results showed a similar linear dependence on the annealing time (Figure 12), but the magnitude of the thickness of the annealed samples is in the range of 25−30 nm, systematically lower than that of the raw data.

The broadening of the intermixing layer, as correctly pointed out by Sauer and Walsh,[20] was due to the velocity differential of the two planes A and B depicted in Figure 5. The velocity of plane A was controlled by the rate of plasticization of the PPO chains, a process characterized by case II diffusion. The velocity of plane B, on the other hand, was mass exchange of the fully plasticized PPO and the rubbery PS chains. This mass exchange, controlled by Fickean diffusion process, slowed eventually due to the substantial decrease of chemical potential difference across plane B. While the velocity of plane A was approximately constant with time since the PPO concentration at the plane A is fixed at 99% according to the definition of plane A. The intermixing layer broadening reflected variation of the interfacial concentration profile with time, which also caused shifting of the Matano interface relative *to* plane A. At short diffusion times when the interface broadening was negligible the Matano interface moved almost in synchronization with that of plane A, demonstrating a case II diffusion characteristic. At long diffusion times, however, the Matano interface, increasingly influenced by the slow of plane B, moved in fashion more and more like Fickean diffusion. This long time behavior is shown in Figure 4a where a $t^{1/2}$ characteristic can be resolved. The planes A and B as well as the Matano interface of a 90KPS/PPO sample annealing at 433 K for various times are shown in Figure 13a−c. As shown in the figures, the Matano interface moved toward plane B and further from plane A as annealing time increased, confirming that the Matano interface eventually was dominated by the movement of plane B when the diffusion times became large. Finally, the PS/PPO interface can be regarded as an isotropic chemical discontinuity in a solid. The broadening of this interface in fact was a classical problem previously treated by Cahn and Hilliard[49] with the considerations of concentration fluctuation effects. It had been concluded by them that the interface would eventually broaden even in the absence of variation of chemical potential difference across the interface. Exploration along this direction of the interface broadening, however, would require more experiments on various types of polymer interfaces.

In comparison to the theoretical calculations of the slow theory and fast theory, the predictions of the slow theory bear a much better agreement with our experimental data here. However, this result of the glass−rubbery interdiffusion should not be regarded as a proof leading to the final jurisdiction on the "slow vs fast" theories arguments in polymer melts. One should also note that the data used for calculating the mutual diffusivities here are short time diffusion results, which correspond to the interface movement governed by case II diffusion.

In our analysis, the degree of plasticization of the glassy molecules at the interface, quantified as the local glass transition temperature, is important as only the fully plasticized chains with an effective T_g lower than the annealing temperature are capable of crossing the interface into the rubbery PS bulk. Although this approach seems appropriate for short and ordinary diffusion times, for exceedingly long diffusion times, e.g. 310 h at 433 K for PS(90K)/PPO (Figure 10), the interdiffusion continued to proceed even as the effective T_g of the intermixing layer became greater than the annealing temperature. This somehow surprising observation, nevertheless, may stem from the fact that the PPO sample used in this experiment was not monodisperse. The low molecular weight fraction of the PPO molecules could have been fully plasticized at an earlier stage so that the Fickean permeation into the PS layer

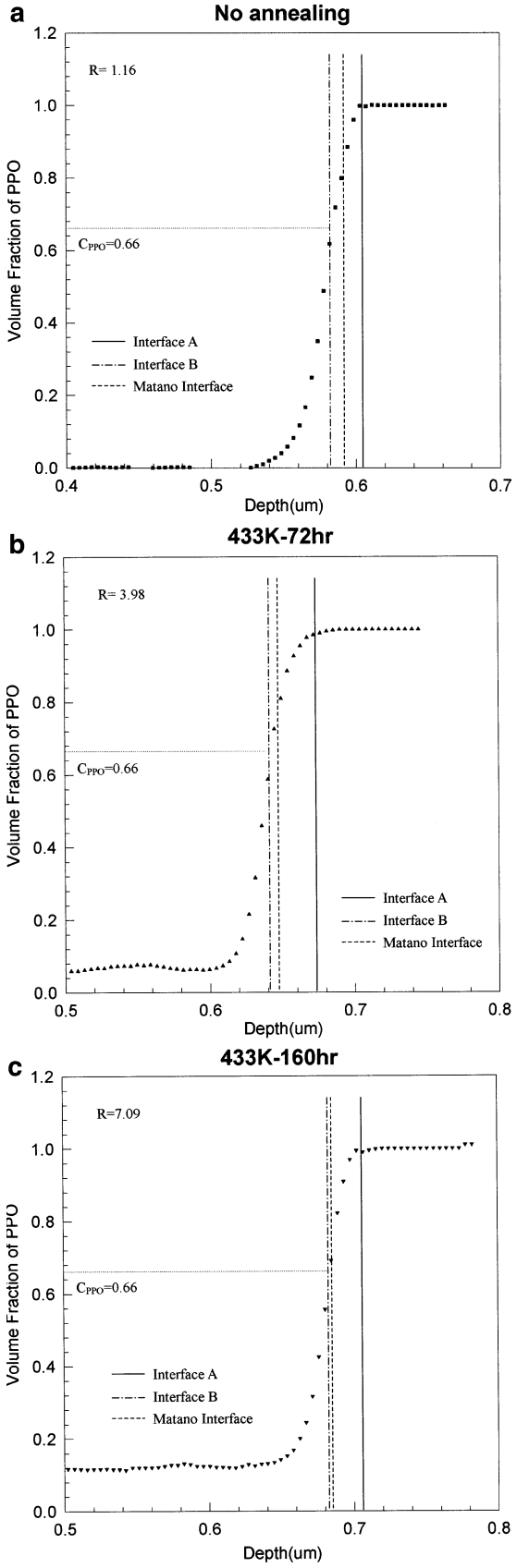

Figure 13. Positions of the Matano interface, planes A and B in the depth concentration profile of the 90KPS/PPO samples annealed at 433 K for various periods of time. The parmeter ***R*** is defined as the ratio of the distance from plane A to the Matano interface to that from plane B to the Matano interface. An increasing ***R*** indicates a moving Matano interface toward plane B: (a) no annealing, ***R*** = 1.16; (b) 72 h, ***R*** = 3.98; (c) 160 h, ***R*** = 7.09.

could start. However, more thorough experiments for long diffusion times are needed to further clarify the intriguing "glassy−glassy" interdiffusion phenomenon.

Conclusions

The interdiffusion and microstructure at a glassy−rubbery interface in a PS/PPO diffusion couple were examined in details in the depth-resolved SIMS experiments. The concentration profile at the glassy−rubbery interface was very different from that of the rubbery−rubbery interfaces. The concentration profile was very sharp with a thickness on the order of 30 nm. The interfacial layer can be divided into a rubbery region and a glassy region according to the local T_g. The glassy−rubbery interface of the diffusion pair moved toward the PPO region upon annealing and the interfacial layer slowly broadened as the diffusion time increased. The polymer interdiffusion across the glassy−rubbery interface simultaneously demonstrates the Fickean and the case II diffusion characteristics. The case II characteristic dominates on the glassy side of the interface where chain mass flow requires plasticization of the glassy polymers by the neighboring rubbery chains. The Fickean characteristic, on the other hand, prevails on the rubbery side of the interface where polymers at both sides of the interface are rubbery chains. The effect of temperature on the interdiffusion was in good agreement with that predicted by the WLF equation. The interdiffusion was strongly influenced by the molecular weight of the PS region. The velocity of the interface decreased with the PS molecular weight according to a negative power law in each of the two molecular weight regimes divided by the critical molecular weight of PS (M_c = 38K). The exponents of the power law dependence, however, are different for the two regimes divided by the M_c. Finally, the mutual diffusion coefficients were calculated from the SIMS data. When the results were compared with those calculated using the fast and slow theories, the slow theory apparently had a much better fit with the experimental results, consistent with the observation that only when the glassy PPO chains at the interface were plasticized could the interdiffusion across the interface subsequently occur.

Acknowledgment. We greatly appreciate the financial support by the National Science Council of Taiwan. The reviewers' constructive comments are also greatly appreciated.

References and Notes

(1) de Gennes, P.-G. *J. Chem. Phys.* **1971**, *55*, 572.
(2) Doi, M.; Edwards, S. F. *J. Chem. Soc, Faraday Trans.* **1978**, *2*, 1789.
(3) Klein, J. *Nature (London)* **1978**, *271*, 143.
(4) Klein, J. *Nature (London)* **1978**, *9*, 217.
(5) Tirrell, M. *Rubber Chem. Technol.* **1984**, *57*, 523.
(6) Crank, J.; Park, G. S. *Diffusion in Polymers*; Academic Press: London, 1968.
(7) de Gennes, P.-G. *Scaling Concept of Polymer Physics*; Cornell University Press: Ithaca, NY, 1979.
(8) Thomas, N. L.; Windle, A. H. *Polymer* **1982**, *23*, 529.
(9) Brochard, F.; Jouffroy, J.; Levinson, P. *Macromolecules* **1983**, *16*, 1638.
(10) Binder, K. *J. Chem. Phys.* **1983**, *79*, 6387.
(11) Sillescu, H. *Makromol. Chem., Rapid Commun.* **1984**, *5*, 519.
(12) Sillescu, H. *Makromol. Chem., Rapid Commun.* **1987**, *8*, 393.
(13) Green, P. F.; Kramer, E. J. *Polymer* **1984**, *25*, 473.
(14) Green, P. F.; Kramer, E. J. *Phys. Rev. Lett.* **1984**, *53*, 2145.
(15) Green, P. F.; Kramer, E. J. *Macromolecules* **1985**, *18*, 501.

(16) Lasky, R. C.; Kramer, E. J. *J. Appl. Phys.* **1987**, *61*, 5137.
(17) Kramer, E. J.*Nature (London)* **1987**, *328*, 234.
(18) Composto, R. J.; Kramer, E. J. *Macromolecules* **1988**, *21*, 2580.
(19) Composto, R. J.; Kramer, E. J. *J. Mater. Sci.* **1991**, *26*, 2815.
(20) Sauer, B. B.; Walsh, D. J. *Macromolecules* **1991**, *24*, 5948.
(21) Wool, R. P. *Macromolecules* **1989**, *22*, 2648.
(22) Wool, R. P.; Whitlow, S. J. *Macromolecules* **1991**, *24*, 5926.
(23) Kramer, E. J. *Macromolecules* **1992**, *25*, 4167.
(24) Narasimhan, B.; Peppas, N. A. *J. Polym. Sci. Part B* **1996**, *34*, 947.
(25) Jabbari, E.; Peppas N. A. *Polymer* **1995**, *36*, 575.
(26) Ho, D. L.; Briber, R. M.; R. L. Jones; Kumar, S. K.; Russell, T. P. *Macromolecules* **1998**, *31*, 9247.
(27) de Gennes, P.-G. *Europhys. Lett.* **1986**, *1*, 221.
(28) Shearmur, T. E.; Clough, A. S.; Drew, D. W.; van der Grinten, M. G. D.; Jones, R. A. L. *Macromolecules* **1996**, *29*, 7269.
(29) Russell, T. P. *J. Polym. Sci., Part B* **1996**, *34*, 2919.
(30) Klein, J. *Macromolecules* **1993**, *26*, 3858.
(31) Green, P. F. *Macromolecules* **1991**, *24*, 3377.
(32) Kramer, E. J.; Russell, T. P. *Macromolecules* **1996**, *29*, 2580.
(33) Edwards, D. A. *J. Polym. Sci., Part B* **1996**, *34*, 981.
(34) Jones, R. A.; Klein, J.; Donald, A. M. *Nature* **1986**, *321*, 161.
(35) Pu, Y.; Rafailovich, M. H. *Macromolecules* **2001**, *34*, 4972.
(36) Pu, Y.; Rafailovich, M. H. *Macromolecules* **2001**, *34*, 8518.
(37) Yokoyama, H.; Rafailovich, M. H.*Macromolecules* **1998**, *31*, 8826.
(38) Vickerman, J. C.; Brown, A.; Reed, N. M. *Secondary Ion Mass Spectrometry principle & application*; Clarendon Press, Oxford, England, 1989.
(39) Wilson, R. G.; Stevie, F. A.; Magee, C. W. *Secondary Ion Mass Spectroscopy-A practical handbook for depth profiling*; A Wiley-Interscience Publication: New York, 1988.
(40) Barrer, R. M. *Trans. Faraday Soc.* **1939**, *35*, 628.
(41) Moore, L. *Br. J. Appl. Phys.* **1968**, *1*, 237.
(42) Werner, H. W. *Surf. Interface Anal.* **1982**, *4*, 1.
(43) Werner, H. W. *Vacuum* **1974**, *24*, 493.
(44) Cowie, J. M.; Harris, G.; S. *Macromolecules* **1999**, *32*, 4430.
(45) Brandrup, J.; Immergut, E. H. *Polymer Handbook*, 3rd ed.; Wiley-Interscience Publication: New York, 1989.
(46) Reed-Hill, R. E. *Physical Metallurgy Principles*, 3rd ed., PWS−KENT Publish Co.: 1986.
(47) Crank, J. *The Mathematics of Diffusion*; Oxford University Press: London, 1975.
(48) Kramer, E. J. *Adv. Polym. Sci.* **1983**, *52/53*, 1.
(49) Cahn, J. W.; Hilliard, J. E. *J. Chem. Phys.* **1958**, *28*, 258.

MA020292J